Bulletin of the Geological Society of Malaysia, Volume 79, May 2025, pp. 101 - 113
DOI: https://doi.org/10.7186/bgsm79202509

Static reservoir characterization of shallow marine carbonate rocks: A case study from the Late Triassic-Early Jurassic Sarki Formation, NE Iraq

Edris M. Pirot[1], Bzhar A. Delizy[1], Irfan Sh. Asaad[2,3,*], Mahdi M. Mamash[1], Maha M. Al-Dabagh[4]

[1] Petroleum Geoscience Department, Faculty of Science, Soran University, Iraqi-Kurdistan Region, Iraq 44008
[2] Earth Sciences and Petroleum Department, College of Science, Salahaddin University-Erbil, Kurdistan Region, Iraq, 44002
[3] Department of Petroleum Engineering, College of Engineering, Knowledge University, Erbil, Iraq, 44001
[4] Petroleum Reservoir Engineering Department, College of Petroleum and Mining Engineering, University of Mosul, Iraq, 41002
*Corresponding author email address: irfan.asaad@su.edu.krd

Abstract: This study investigates the reservoir properties of the Late Triassic-Early Jurassic shallow marine carbonate Sarki Formation outcrop, specifically in the Zarwan section of northeastern Iraqi Kurdistan. The lithology of the studied section comprises dolomite, dolomitic limestone, recrystallized breccia and thin beds of marls, with a formation thickness of approximately 115 m. Various techniques, including microscopic study, core plug analysis and scanning electron microscopy (SEM) were employed to assess reservoir properties. The Sarki Formation consists of diverse pore types, including vuggy, moldic, intraparticle, interparticle, fracture, intercrystalline, stylolitic and microporosity. Identified diagenetic processes include early dolomitization, compaction (physical and chemical), cementation (granular, blocky, and drusy cements), micritization, dissolution, silicification, neomorphism, late dolomitization, and fracturing. Petrographic analysis indicated a porosity average of 2% in the lower part of the formation and 6% and 9.5% in the middle and upper parts, respectively. A scanning electron microscopy (SEM) study confirmed similar porosity values with micropore sizes in the studied section. Core plug analysis results were roughly aligned with optical assessments, revealing porosity values of 2%, 6%, and 10% for the lower, middle, and upper parts, respectively. Overall, the Sarki Formation exhibited negligible to fair porosity ranges. Permeability measurements values averaged 0.01 md, 0.02 md, and 0.13 md for the lower, middle, and upper parts respectively, indicating a poor to fair permeability range. The upper part of the formation was deemed to have fair reservoir quality due to fewer observed diagenetic processes than the middle and lower parts, although permeability may be relatively low. In contrast, the lower and middle parts displayed poor reservoir characteristics, suggesting limited potential in the context of the petroleum reservoir.

Keywords: Reservoir characterization, Sarki Formation, Early Jurassic, porosity, permeability, Northern Iraq

INTRODUCTION

The static reservoir characterization of shallow marine carbonate rocks is crucial for understanding subsurface geology, particularly in hydrocarbon exploration. It involves a description of the structure, thickness, lithology, porosity, facies, permeability, and initial fluids in the reservoir. Rock porosity refers to the percentage of void spaces or openings within a rock formation. Rock permeability is the ability of a rock to allow fluids (such as water and oil) to pass through its pore spaces (North, 1985). It measures the ease with which fluids can flow within the rock, influencing the movement and extraction of substances in subsurface environments, such as petroleum reservoirs or aquifers (North, 1985).

The Sarki Formation was initially defined by Dunnington 1952, in Bellen *et al.* (1959) at its type locality in the Chia Gara Mountain, south of Amadyia, northern Iraq. Its thickness varies across different locations, with an estimation of 300 m at the type locality (180 m for the upper part and 120 m for the lower part). The total thickness of the Sarki Formation in the studied area is 115 m, comprising dolomite, dolomitic limestone, and recrystallized breccia. Its notable development is extensively exposed in the High Folded, Imbricated, and Northern Thrust zones of Iraq (Buday, 1980). Given the scarcity of fossils and the absence of age-diagnostic features, the age of the Sarki Formation was determined based on its stratigraphic position. It is positioned above the Late Triassic (Carnian-Norian) Baluti Formation and below the Late Liassic Sehkaniyan Formation, indicating a Rhaetian-Sinemurian age (Lunn *et al.*, 2019; Mohialdeen *et al.*, 2022). The Butmah Formation is the lateral equivalent of the Sarki

0126-6187; 2637-109X / Published by the Geological Society of Malaysia.

Formation in Central Iraq, whereas the Ubaid Formation is the equivalent of it in the Western Desert (Buday, 1980). In surrounding countries, it is equivalent to the Neryiz Formation in Iran, and it is equivalent to the upper part of the Dolaa Group in central Syria (Jassim *et al.*, 2006). Previous studies have focused on lithology, stratigraphy, and depositional environments of Sarki Formation but have done little on reservoir quality. Dunnington (1958) initially described the Sarki Formation, assigning the name to a dolomite-limestone complex in the Chia Gara Mountain range in the High Folded Zone of northern Iraq. Bellen *et al.* (1959) published comprehensive information about Jurassic formations, introducing the term Sarki for this formation. Their study focused on lithology, stratigraphy, bio-contents, and the depositional environment based on a section at Chia Gara Mountain. Buday (1980) provided a detailed description of the Sarki Formation, especially in terms of the lithology and depositional environment of the type locality. Surdashy (1999) concluded that the Sarki Formation's age is restricted to early Jurassic stages. He indicated deposition in open platforms, oolitic shoals, and deep shelf basins. Jassim *et al.* (2006) used information from Bellen *et al.* (1959) and Buday (1980) to support their findings. They used tectonic and isopach maps and information about the location and tectonic settings of the Liassic sequence zone where the Sarki Formation was deposited to back up their findings. According to Al-Badry's (2012) study of the stratigraphy and geochemistry of Jurassic formations in the Gely-Derash and Banik areas, the Sarki Formation was formed on tidal flats, in Sabkha, and in lagoons. Al-Juboury & McCann (2015) defined the petrology and geochemical interpretation of the Triassic and Jurassic boundaries in northern Iraq. The presence of suture mosaic dolomite, which indicates deposition between the seafloor and the atmosphere, led them to believe that the lower part of the Sarki Formation formed in a shallow marine environment. Delizy & Shingaly (2022) identified the main diagenetic processes that affect the carbonate rocks of the Sarki Formation. These processes include dolomitization, compaction, cementation, micritization, solution, and silicification. They concluded that depositional environments involve peritidal zones, lagoons, and high-energy carbonate shoals. Omar *et al.* (2023) study of the paleoclimate, paleosalinity, and paleoredox conditions of the Lower Jurassic-Lower Cretaceous sediments in northeastern Iraq. The Butmah Formation, which is equivalent to the Sarki Formation, is considered to be poor source rock with TOC content 0.44 wt.% with Tmax of 28°C in well Zab-1 in northern Iraq (Abdula, 2016). In contrast, it exhibits good reservoir characterizations, especially in the Shaikan 5B Well. However, the poor effective porosity and permeability in the formation at other sites are attributed to the presence of shale thin beds and cements, especially anhydrite cement (Al-Dabagh & Asaad, 2025).

The analysis of outcrop sections can offer valuable insights into geological and petrophysical properties, which are often challenging and costly to obtain from subsurface data. When geologists look at an outcrop's geometric, sedimentary, and petrophysical features in detail, they can learn useful information that can help them explore and develop subsurface reservoirs. This article delves into a comprehensive case study focused on the Upper Triassic-Lower Jurassic Sarki Formation from the outcrop due to limited subsurface well data, situated in the northeastern Iraqi Kurdistan region. Therefore, the current work aims to study the static reservoir properties of the Sarki Formation at the Zarwan outcrop section in the Rawanduz area to comprehend the distribution of hydrocarbons and connectivity of the reservoir.

GEOLOGICAL SETTING

In the northern and northeastern parts of Iraq, within the High Folded Zone and Imbricated Zone, the Upper Triassic-Liassic sequence is visible in several anticlines (Jassim *et al.*, 2006). The Sarki Formation is widely exposed at the cores and limbs of several anticlines in Imbrication and Northern Thrust Zone of Iraq. For this study, Zarwan section located 500 m to the north of Zarwan Village, about 15 km northeastern Rawanduz District in Erbil Governorate, at Lat. 36° 38' 44"N and Long. 44° 39' 53"E (Figure 1A) was selected. The studied section is exposed at the northeastern limb of the asymmetrical Spibalies Anticline in Imbrication Zone with the fold axis trending NW-SE (Balaki, 2004). The anticline is double plunging, around 26 km in length with varying dip angles on its limbs, the NE limb dips at a steep angle and the SW limb dips approximately 50° (Delizy & Shingaly, 2022). The Upper Triassic-Lower Jurassic formations (Sarki & Sehkaniyan) formed the core of the anticline. While Cretaceous rocks formed the limbs of the anticline and are represented by the Balambo, Qamchuqa, and Tanjero formations (Figure 1B).

The thickness of the Sarki Formation in the Zarwan section is 115 m, and its lithologically comprises dolomite, dolomitic limestone, recrystallized breccia, and thin bedded grey marlstone (Figure 2). The upper contact of the Sarki Formation is with the Sehkaniyan Formation (Figure 3A) and the lower contact of the formation is not exposed and covered in the selected section, which is supposed to overlie the upper Triassic Baluti Formation, because it is visible in the Warte area southeast of Zarwan Village (Asaad *et al*., 2021). The lower part of the formation consists of medium- to thick-bedded dolomitic limestone and brecciated dolomitic limestone (Figures 3B & C). The middle part comprises of thin bedded of dolomitic limestone with a thin grey bedded of marlstone (Figure 3D). The upper part is composed of thin to medium, highly fractured dolomite (Figure 3E).

METHODS AND MATERIALS

Field work and sample collection

Due to the difficulty of obtaining comprehensive subsurface data in Kurdistan and Iraq, the surface outcrop of the Sarki Formation in the Zerwan area was chosen for the

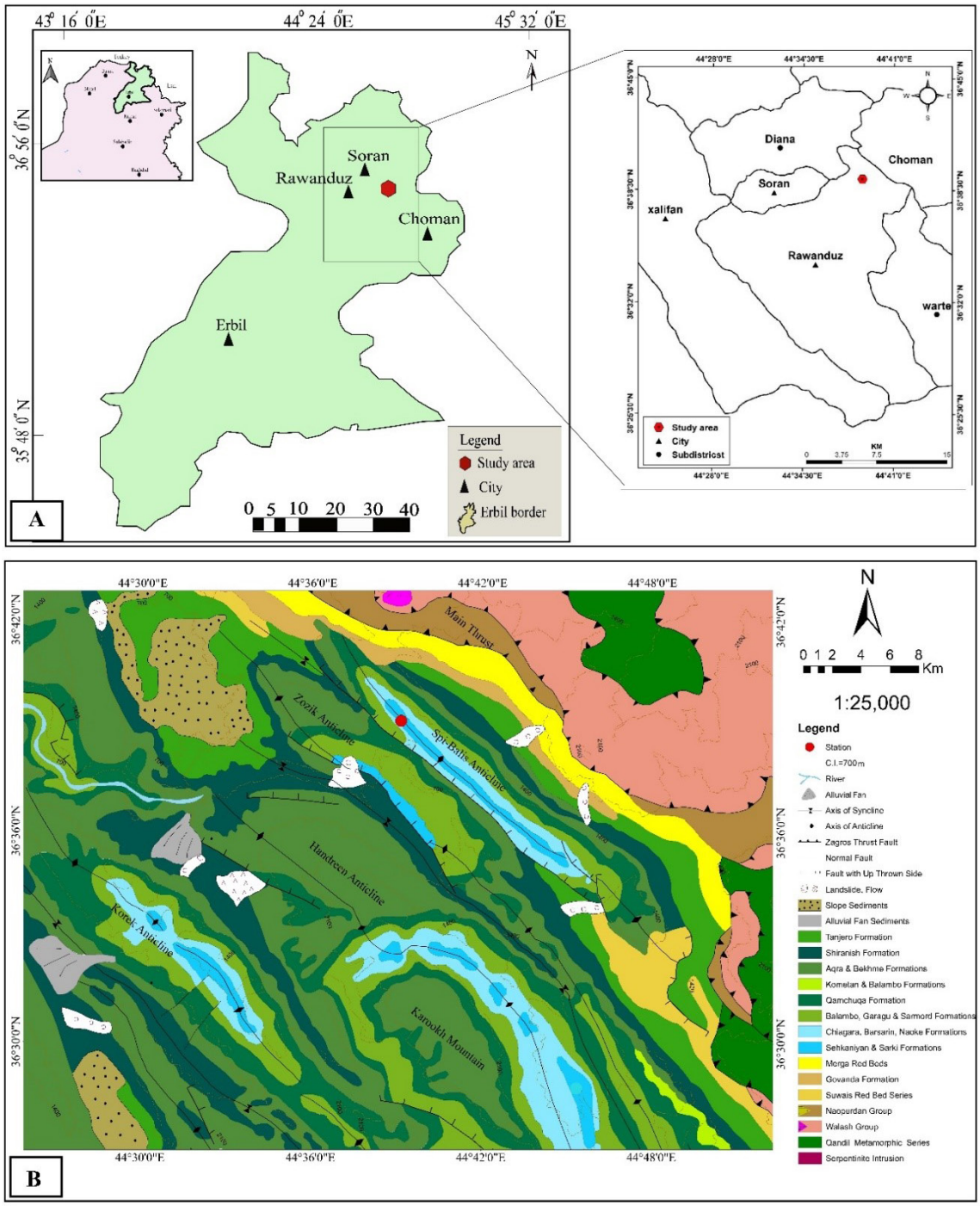

Figure1: A) Location map of the Zarwan section. **B)** Geological map of the studied sections (after Sissakian, 2000; Delizy & Shingaly, 2022).

current study. A detailed fieldwork was carried out in order to describe the nature of selected outcrop and collecting samples. The field work was done on October 7, 2023, using geologic hummers, meter measuring tape, and hand lenses in addition to dilute HCl for distinguishing between calcite and dolomite. The section was described and logged in details. The sum of 36 carbonate samples was collected from studied section. The samples were collected at every change in lithology or color (random sampling). The upper and lower parts of each sample were marked. The collected samples were used for various experiments including normal thin section and covered with blue risen, core samples and SEM analysis.

Thin sections preparation

The special type of thin sections impregnated with blue dyed e-poxy were prepared in Metallurgy and Material

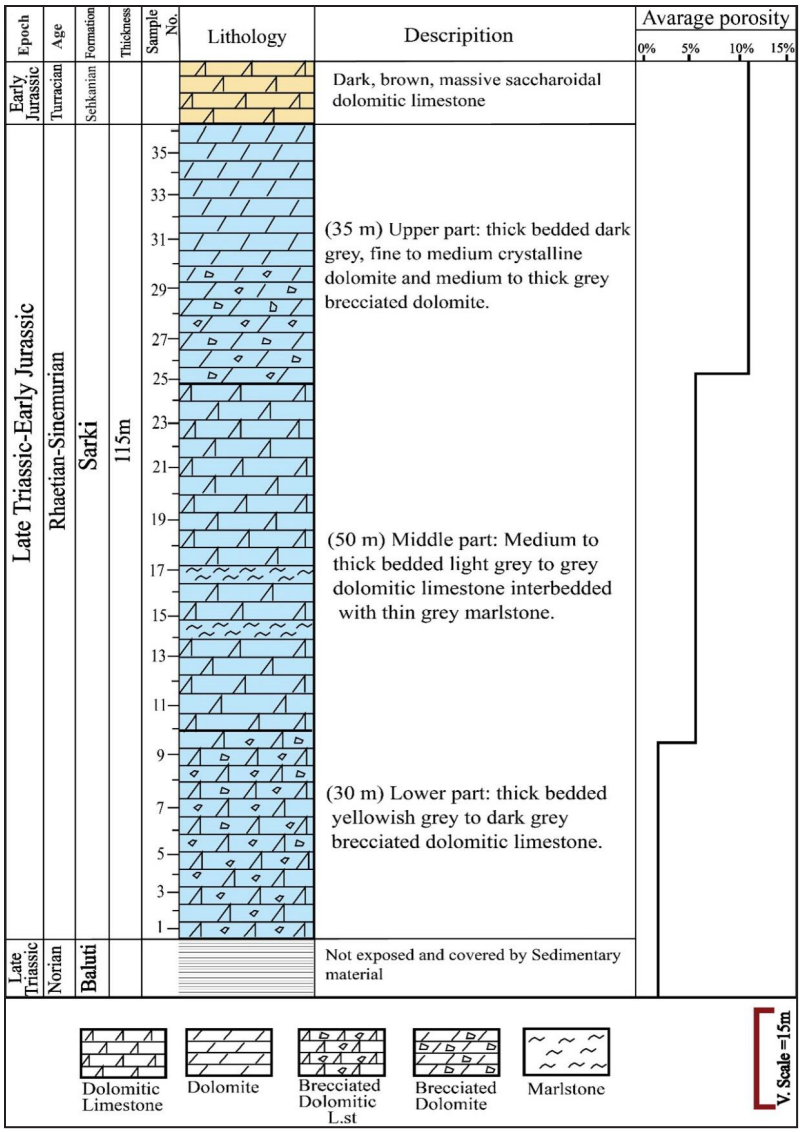

Figure 2: Stratigraphic column with average porosity of the Sarki Formation (Late Triassic- Early Jurassic) in Zarwan section, northern Iraq.

Engineering Lab, of Tehran University, Tehran, Iran to highlight pore areas, which locates the pores in blue and separates them from the surrounding components. This helps to detect porous areas precisely when taking thin section images and importing them into Digimizer and ImageJ software. This software was used to determine the types and sizes of pores and, consequently, the percentage of porosities. Additionally, normal thin sections were also prepared in the same laboratory.

Scanning Electron Microscope (SEM)

Scanning Electron Microscopy (SEM) was used in order to identify different types of porosity and the degree of connectivity between the pores. SEM analysis was performed with 190 scanning electron microscopy (SEM; QUANTA 450) coupled with energy dispersive X-ray 191 spectroscopy (EDS; BRUKER-QUANTAX). Samples were coated with gold to enhance image resolution. The process of SEM analysis was done by properties of measurement. Standard conditions standard included HV setting of 5kv, 12.50kv and 20 kv, a spot size of 4.5, High vacuum mode, det (ETD), and a counting time of 20 second per element for each test.

Petrographic image analysis (PIA)

ImageJ software was used to estimate porosity from the studied thin sections that treated with blue epoxy. The process of estimation of porosity is briefly given herein: After opening ImageJ software and the JROP tool from toolbar of ImageJ was selected. JPOR would ask to identify images of a thin section that had been treated with blue epoxy. Eight or 16 bits would then be chosen for each image. The threshold would then be applied to the pictures of each thin section by following the directions that would appear in the toolbar of the pop-up window (Image – Adjust – Threshold). The aim is to threshold these various colors separately and

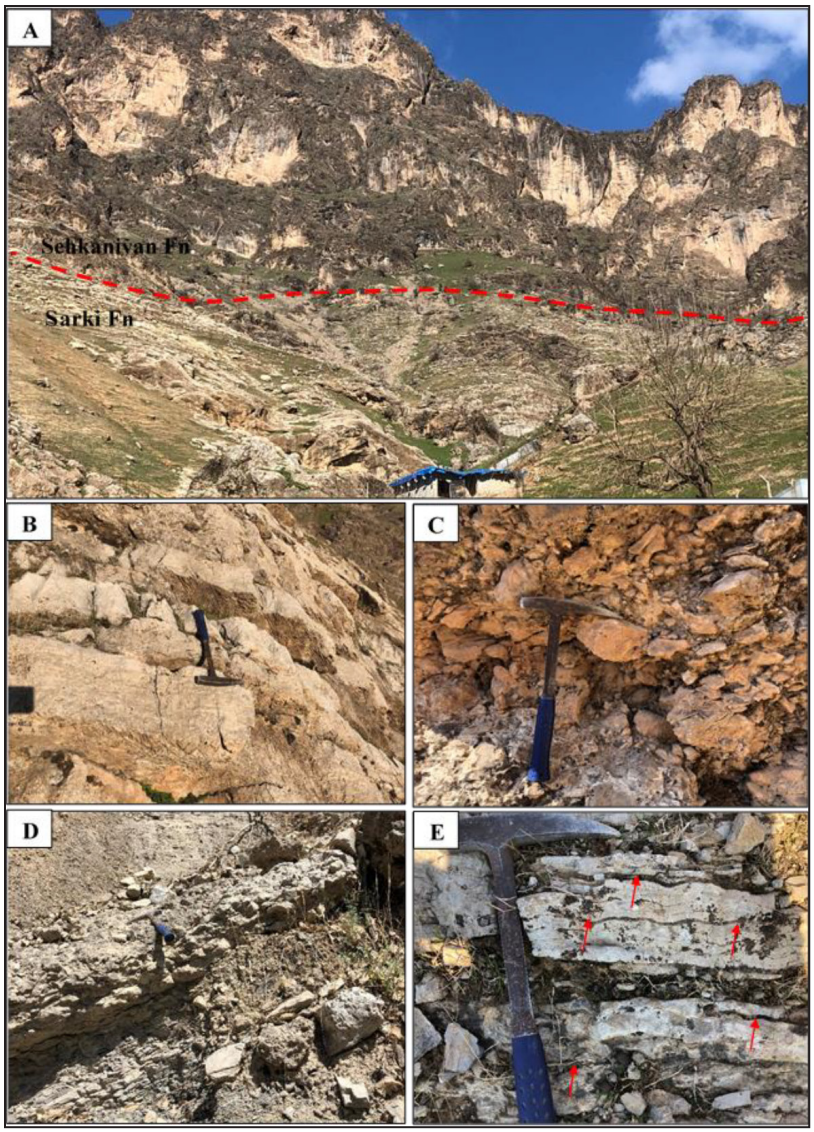

Figure 3: Field photographs showing: **A)** Sarki Formation with overlying Sehkaniyan Formation at the Zarwan section. **B)** Medium to thick bedded, fractured, hard dolomitic limestone from lower part. **C)** Brecciated dolomitic limestone from lower part of the Sarki Formation at the Zarwan section. **D)** Thin bedded of compacted marlstone from middle part of the formation. **E)** Thin to medium bedded, highly fractured dolomite from upper part of the formation (arrows).

add them together in order to measure the average porosity present in each image from each thin section. After threshold process was done for each image, porosity measurement was done by analyzing process for each thin section, in the toolbar (Analyze-Measure). To obtain a reasonable value of porosity an average of 25 images per thin section was analyzed. The permeability is also detected through thin sections (Figures 4 and 5). This method provides a reliable estimate of porosity, consistent with SEM analysis.

RESULTS AND DISCUSSION

Petrographic image analysis (PIA)

Petrographic image analysis (PIA) is a widely employed technique for examining and quantifying the shape, size, and estimated values of porosity (Ehrlich, *et al.*, 1984; Anselmetti, *et al.,* 1998; Albeyati *et al.*, 2021). The present study show that the common pore types in the Sarki Formation include intraparticle and microporosity in the lower part, vuggy, intraparticle, and stylolitic pores in the middle part and vuggy, interparticle, intraparticle, microporosity, fracture and intercrystalline pores and in the upper part (Figures 5 and 6). Table 1 presents porosity values for different parts of the Sarki Formation, utilizing images taken by a Leica Microscope with both normal and special thin sections, as well as Scanning Electron Microscope (SEM). Based on the study of normal, special, and SEM images with ImageJ software, the porosity values for the Zarwan section range from 1% to 11.5%. The lower part ranges from 0.5% to 3.5%, averaging 2%. The middle part ranges from 6% to 7.5%, averaging 6%. The upper part ranges from 8% to 11.5%, with an average of 10% (Figure 4 and Table 1). The examination of porosity using the Scanning Electron Microscope (SEM) analysis conforms porosity values and types consistent with those obtained through ImageJ and Digimizer software. Porosity values obtained from normal and special thin sections using the Leica Microscope are generally similar

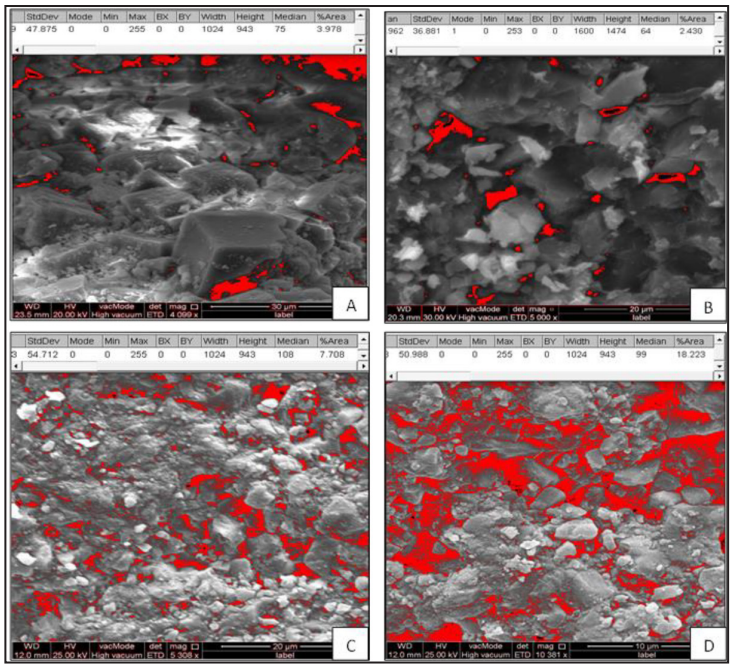

Figure 4: (A) Porosity percentage measurement steps by ImageJ software in a SEM captured image from lower part of Sarki Formation about 4%. **(B)** Porosity percentage measurement steps by ImageJ software in a SEM captured image from the lower part of Sarki Formation about 2.5%. **(C)** Porosity percentage measurement steps by ImageJ software in a SEM captured image from the middle part of Sarki Formation about 8%. **(D)** Porosity percentage measurement steps by ImageJ software in a SEM captured image from the upper part of Sarki Formation about 10%. (Red color is porosity area).

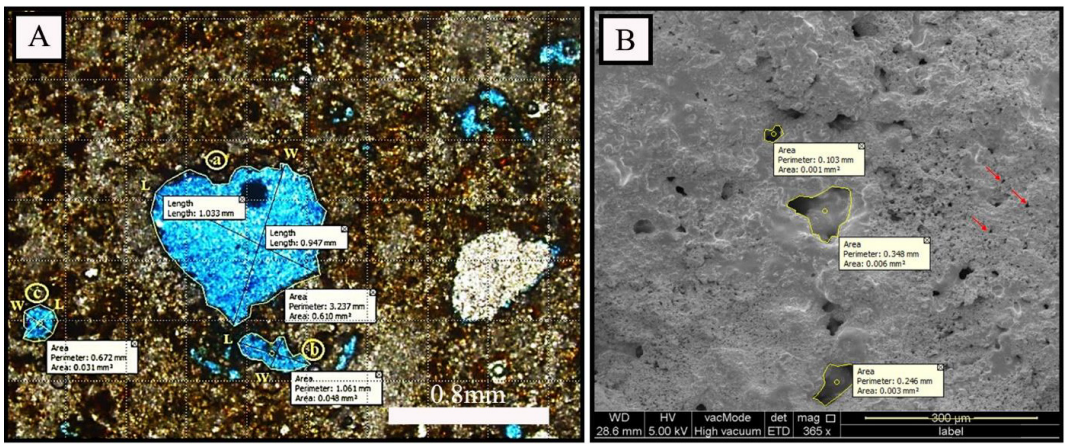

Figure 5: Porosity percentage measurement by Digimizer Software: **(A)** Measurement of vug porosity size by Digimizer software in a thin section captured image. *L=Length and W=Width of porosity. (a) Large vuggy porosity. (b and c) Medium vuggy porosity. **(B)** Measurement of porosity size by Digimizer software in a SEM captured image, microporosity (red arrows).

to SEM measurements, indicating agreement between the techniques. There is variability in porosity values among samples within each part of the formation, which could be attributed to geological and technical heterogeneity (Pirot & Edilbi, 2022). Porosity values suggest negligible to poor reservoir quality in the lower part, fair reservoir quality in the middle part, and fair reservoir quality in the upper part based on Choquette & Pray (1970) classification.

Variations in pore size within the depositional rock fabric are influenced by crystal and grain size groupings. These pores are categorized as mesopores, with small sizes ranging from 1/16 mm to 1/2 mm and large sizes from

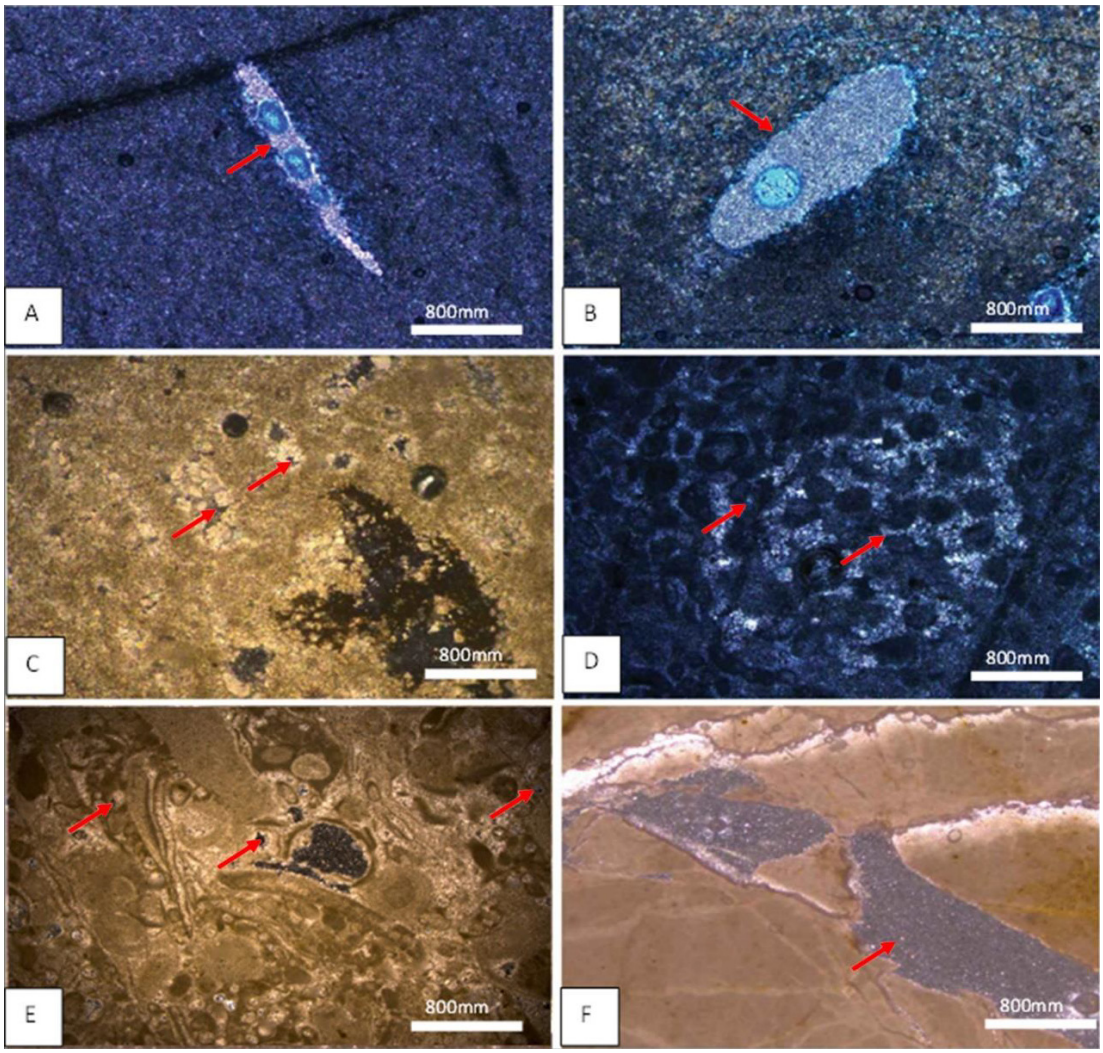

Figure 6: Porosity types from different parts of Sarki Formation: **(A)** Moldic porosity, from the middle part of the formation (arrow). **(B)** Vuggy porosity, from the upper part of the formation (arrow). **(C)** Intercrystalline porosity, from the upper part of the formation (arrows). **(D)** Interparticle porosity, from the upper part of the formation (arrows). **(E)** Intraparticle porosity, from the lower part of the formation (arrows). **(F)** Fracture porosity, from the upper part of the formation (arrow).

1/2 mm to 4 mm. Additionally, mega-pores are further divided into small sizes (4 mm to 32 mm) and large sizes (32 mm to 256 mm) (Choquette & Pray, 1970). According to Digimizer software analysis, the pores in the Zarwan section are classified as micropores (<1/16, 0.0625 mm²) as the pore areas in the lower part range between 0.0173-0.0237 mm², the middle part between 0.0260-0.0161 mm², and the upper part between 0.0515-0.612 mm².

Furthermore, SEM images reveal porosity sizes consistent with those obtained from thin section studies (Figures 5A and B).

Both ImageJ and Digimizer software tools show similar porosity percentages for the samples, indicating reliability in the measurements regardless of the software used. The consistency in porosity trends across different imaging methods (microscope and SEM) and software tools (ImageJ and Digimizer) enhance the confidence in the results (Pirot & Edilbi, 2022). The upper part of the Sarki Formation exhibits higher porosity values than the lower and middle parts, suggesting greater reservoir potential. Lower porosity in the middle and lower parts suggests reduced reservoir quality, potentially affecting fluid storage and flow.

Diagenetic impact on the porosity

The main diagenetic processes that affected the carbonate rocks from the different parts of the Sarki Formation include early dolomitization, compaction (physical and chemical), cementation (granular cement, blocky cement, and drusy calcite cements), micritization, dissolution, silicification, neomorphism, late dolomitization and fracturing (Figures 7 and 8). The diagenetic processes of dolomitization and dissolution have notably increased the secondary porosity in

Table 1: The correlation porosity values were determined from the images taken by the Leica Microscope for both normal and special thin sections and SEM (Scanning Electron Microscope).

Parts of Sarki Formation	Sample No.	Porosity Types	Porosity by Leica Microscope for normal thin section by ImageJ and Digimizer softwares		Porosity by Leica Microscope for special thin section by ImageJ and Digimizer softwares		Porosity by SEM by ImageJ and Digimizer softwares	
Type of Thin sections			ImageJ	Digimizer	ImageJ	Digimizer	ImageJ	Digimizer
Upper Part	S35	Vuggy, Interparticle, Intraparticle, Microporosity, Fracture and Intercrystal	9.5%	10.0%	11.5%	10.5%	11.5%	11%
	S31	Intercrystal, Vuggy, Microporosity, Fracture and Interparticle	10.0%	10.5%	9.5%	10.0%	11.5%	10.5%
	S27	Interparticle, Intraparticle, Intercrystal, Microporosity and Vuggy	9.0%	9.5%	9.0%	8.5%	9.5%	8.0%
Average			9.5%	10.0%	10%	9.5%	11.0%	10.0%
Middle Part	S24	Intraparticle, Moldic, Vuggy, and Stylolitic	6.0%	7.0%	7.0%	7.5%	7.0%	6.5%
	S19	Intraparticle, Moldic, Vuggy, and Stylolitic	7.0%	6.0%	7.0%	7.0%	6.5%	6.0%
	S15	Moldic, Vuggy, Intraparticle, and Stylolitic	6.0%	6.0%	6.0%	6.5%	6.5%	6.5%
Average			6.0%	6.0%	6.5%	7.0%	6.5%	6%
Lower Part	S11	Microporosity and Intraparticle	2.0%	2.5%	3.0%	2.5%	3.5%	2.5%
	S6	Microporosity and Intraparticle	2.5%	2.0%	3.5%	3.0%	3.0%	3.5%
	S2	Intraparticle and Microporosity	1.0%	1.5%	0.5%	1.0%	1.0%	1.5%
Average			2.0%	2.0%	2.0%	2.0%	2.0%	2.5%

dolostone, dolomitic limestone, and crystallized dolomitic limestone, particularly in intercrystalline, moldic, and vuggy pore spaces (Delizy & Shingaly, 2022). These suggest that diagenesis plays a primary role in shaping pore development, stylolitization and fracturing significantly enhancing reservoir permeability for the upper part of Sarki Formation. However, sometimes the stylolitization aids in decreasing total porosity, but interconnected channels formed can enhance fluid flow within the rock (Fahad *et al*., 2021). The fracturing contributes to the formation of secondary pores (Balaky *et al*., 2023), and facilitates gas and fluid movement within the rock (Jiang *et al.*, 2022). As mentioned earlier, various techniques are employed to assess porosity. Table 2 represent porosity values across different parts of the Sarki Formation along with cementation percentages, distinguishing between total porosity (before cementation), which includes both pore spaces and cemented areas, and effective porosity. The effective porosity is the interconnected pore volume or void space in a rock that able to transmit fluids. The different types of calcite cement (granular, blocky and drusy) filled the pore spaces of the carbonate rocks in the Sarki Formation. Cementation caused in reducing the rocks porosity and this led to reducing permeability (Ahmed *et al*., 2020). The data is crucial in understanding the reservoir quality of the rock samples. The results of data analysis indicate that all parts of the Sarki Formation exhibit poor reservoir quality, characterized by relatively low effective porosity even after accounting for cementation. However, the upper part relatively offers better storage and flow capacity for hydrocarbons than

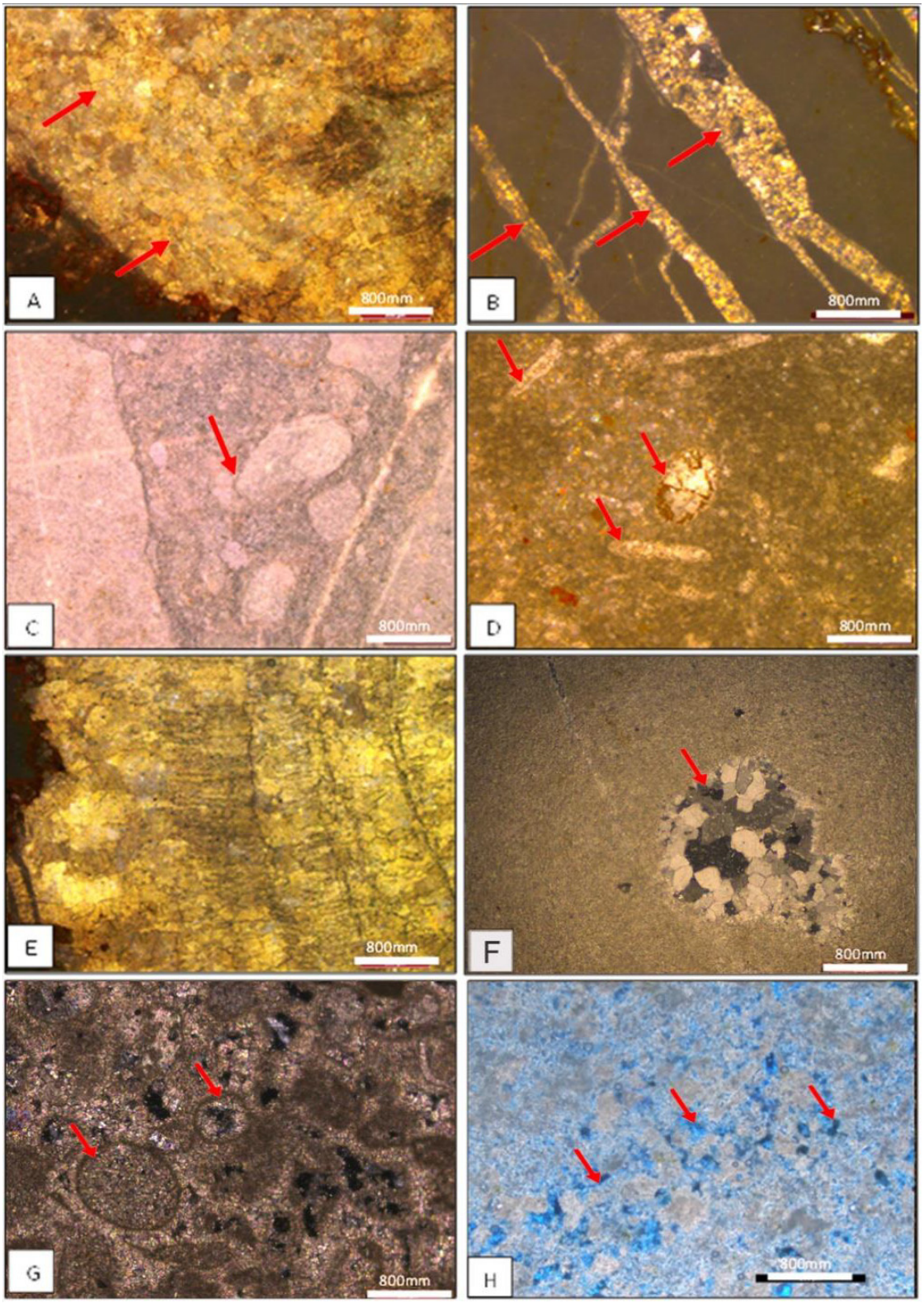

Figure 7: The diagenesis types from different parts of Sarki Formation from Zarwan Section: **(A)** Dolomitization formed medium to coarse crystals (arrows). **(B)** Fracture filled by granular cement (arrows), may indicate strong tectonic and/or deep burial effect. **(C)** Concave-convex contact forming between grains (arrow) due to over close packing on non-skeletal grains. **(D)** Skeletal grains filled by granular cement (arrows). **(E)** Fracture (vein) filled by blocky cement. **(F)** Skeletal grains filled by drusy cement (arrow). **(G)** Micrite envelops around ooid grains filled by dolomite cement (arrows). **(H)** Dissolution formed on the groundmass (arrows).

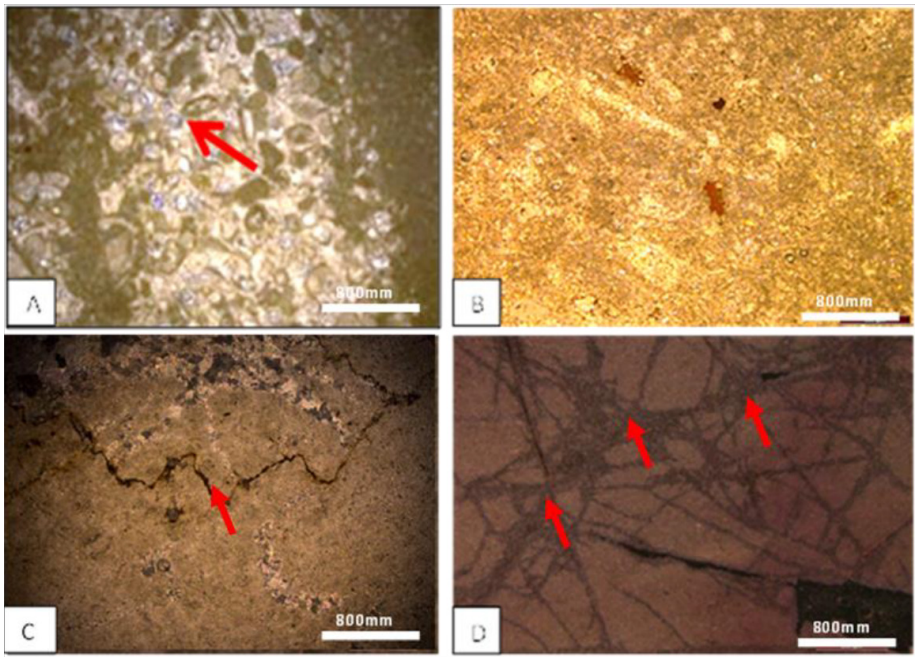

Figure 8: The diagenesis types from different parts of Sarki Formation from Zarwan section: **(A)** Silicification formed on carbonate grains (red arrow) surrounding by ooid and algal mats. **(B)** Neomorphism changed the micritic groundmass to microspar. **(C)** Stylolitic porosity formed by solution, the black color is bitumen filling the remaining space of stylolite (arrow). **(D)** Fracture porosity enlargement by solution processes (arrows).

Table 2: The porosity values were determined for various thin section images from distinct sections of the Sarki Formation, considering both cases of total porosity (%) with cement and effective porosity (%) without cement.

Part of Sarki Formation	Sample No.	Total Porosity (%) with cement	Effective Porosity (%) without cement
Upper Part	S35	11.0%	9.5%
	S31	12.5%	10.0%
	S27	10.0%	8.5%
Average	**S27+S31+S35/3 =**	11.0%	9.0%
Middle Part	S24	11%	7.5%
	S19	8.0%	7.0%
	S15	12.0%	6.0%
Average	**S15+S19+S24/3 =**	10.0%	7.0%
Lower Part	S11	7.5%	4.5%
	S6	6.5%	2.0%
	S2	8.0%	2.5%
Average	**S2+S6+S11/3 =**	7.0%	3.0%

lower and middle parts. The impact of cementation is more pronounced in the middle and lower parts, significantly reducing effective porosity. This suggests that these parts posing challenges for hydrocarbon extraction due to lower porosity and increased cementation.

Porosity is prominent in the different parts in the Sarki Formation, but the high amount of cementation has reduced the permeability. According to rate of flow in pore space, the permeability is higher in interparticle and intercrystalline pores than moldic and intraparticle type (Ahr, 2008). In the dolostone facies of the Saki Formation, the intercrystalline pores are generally interconnected. However, due to interlocking crystals of dolomite, the pore spaces between crystals are not effective for fluid transmission (Figures 9, A and B). Hence, the permeability observed in the studied section is not sufficient t for being high reservoir quality.

Direct methods for measurement of porosity and permeability

The laboratory's direct measurement method for determining porosity and permeability is considered highly reliable. Table 4 presents the analysis of core plugs, indicating porosity values of 2%, 2%, and 3% for the lower part, 6%, 7%, and 6% for the middle part, and 9%, 10%, and 11% for the upper part. The measured porosity values correspond closely to those estimated using ImageJ processing. Specifically, the lower part exhibits negligible porosity, the middle part shows poor porosity, and the upper part displays fair porosity, as detailed in Tables 3 and 4. Notably, all parts of the Sarki Formation, particularly the lower and middle parts, appear to be significantly affected by cementation.

The permeability values range from 0.00md to 0.20md, averaging 0.01md, 0.00md, and 0.02md for the lower part,

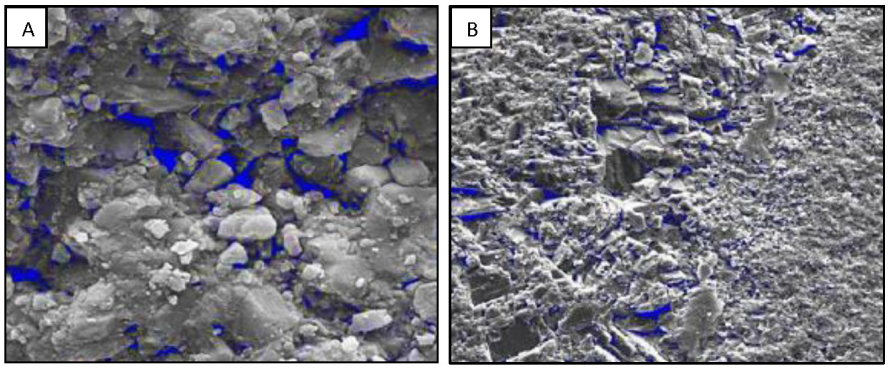

Figure 9: SEM photographs of the Sarki Formation: **(A)** Micro-porosity between particles and very fine crystals of dolomite with low permeability. **(B)** Minor amount of intercrystalline porosity within packing crystals of dolomite with low permeability.

Table 3: Porosity and permeability as indicators of reservoir quality (North, 1985).

Porosity (%)	Reservoir quality	Permeability (Millidarcy)	Reservoir quality
0-5%	Negligible	<1-15	Poor to fair
5-10%	Poor	15-50	Moderate
10-15%	Fair	50-250	Good
15-20%	Good	250-1000	Very Good
20-25%	Very Good	>1000	Excellent

Table 4: The porosity values which are determined by porosimeter instruments and permeability values are determined by the permeameter instrument for the Sarki Formation from the Zarwan Section.

Sarki Formation	Sample No.	Porosity Percentage %	Permeability (md)
Upper Part	SC-35	11%	0.20
	SC-31	10%	0.10
	SC-27	9%	0.10
Average	**SC-27+SC-31+SC-35/3 =**	10%	0.13
Middle Part	SC-24	6%	0.04
	SC-19	7%	0.02
	SC-15	6%	0.01
Average	**SC-15+SC-19+SC-24/3 =**	6%	0.02
Lower Part	SC-11	3%	0.02
	SC-6	2%	0.00
	SC-2	2%	0.01
Average	**SC-2+SC-6+SC-11/3 =**	2%	0.01

0.01md, 0.02md, and 0.04md for the middle part, and 0.10md, 0.10md, and 0.20md for the upper part (Table 4). These permeability values suggest poor to fair permeability characteristics for the analyzed samples, as indicated in Tables (3 and 4). Table 4 and Figure 10 illustrate that the formation can be classified as a reservoir with negligible to fair characteristics based on North (1985) classification.

It is clear from petrographic, SEM, and core plug analysis that the Sarki Formation in the Zarwan section had poor reservoir quality that will consequently affect hydrocarbon production. However, it had a considerable primary porosity, but diagenetic processes diminish its permeability except the upper part, which slightly has fair permeability as revealed by the closeness of total porosity and effective porosity ratios. Poor quality reservoirs present significant challenges to hydrocarbon production. Despite these challenges, various techniques can be employed to improve hydrocarbon recovery from poor quality reservoir as reservoir simulation, waterflood management, and enhanced oil recovery (EOR) techniques.

CONCLUSIONS

In this study, porosity types, rate of porosity and permeability were determined using SEM and thin sections with microscope analysis, supplemented by direct Core Plug Analysis. At the Zarwan section, the Sarki Formation exhibits diverse lithologies, including dolomitic limestone, dolomite, brecciated dolomite, brecciated dolomitic limestone and thin-bedded marl. Petrographic image analysis (PIA) of thin sections indicates that the carbonates of the Sarki were characterized by various types of pores including moldic, vuggy, intraparticle, stylolitic, interparticle, microporosity, fracture and intercrystalline pores. Generally, the cementation reduces porosity and permeability by filling previously dissolved skeletal grains molds and fractures, particularly in the lower and middle parts of the formation. Different types of porosity in the carbonate of the Sarki Formation contribute partially to its reservoir quality, although permeability in the studied section is nearly negligible. The low permeability is primarily due to diagenetic processes such as cementation, compaction and interlocked dolomite crystals. The upper part of the formation is considered to have fair reservoir quality, as it is less diagenesis process compared to the lower and middle parts thought its permeability may still be low. Therefore, the lower and middle parts of the formation in the studied section exhibit poor sufficient reservoir characteristic warranting concern from the standpoint of the petroleum system, however, the upper part may be considered to have fair reservoir quality. The poor-quality reservoir of the formation poses significant challenges to hydrocarbon productivity. However, productivity may be increased and more hydrocarbons can be recovered with the right methods and technologies.

ACKNOWLEDGEMENT

The authors send their appreciation to Mr. Payman Aspoka from Research Center of Soran University, for his help of laboratory facilities. We are grateful to Dana Noory Ridha, Ph.D. from University of Birmingham, for his proofreading of the manuscript. The anonymous reviewers are thanked for their constructive comments.

AUTHORS CONTRIBUTION

EMP performed analysis, conducted result interpretation and wrote the first draft of the manuscript. BAD collected field data and wrote the manuscript. ISA reviewed the manuscript and improved their interpretation. MMM collected field data. MMA improved the final draft of the manuscript.

CONFLICT OF INTEREST

The authors have no conflicts of interest to declare that are relevant to the content of this article.

REFERENCES

Abdula, R.A., 2016. Organic geochemical assessment of Jurassic potential source rock from Zab-1 Well, Iraqi Kurdistan. Iraqi Bulletin of Geology and Mining, 12(3), 53-64.

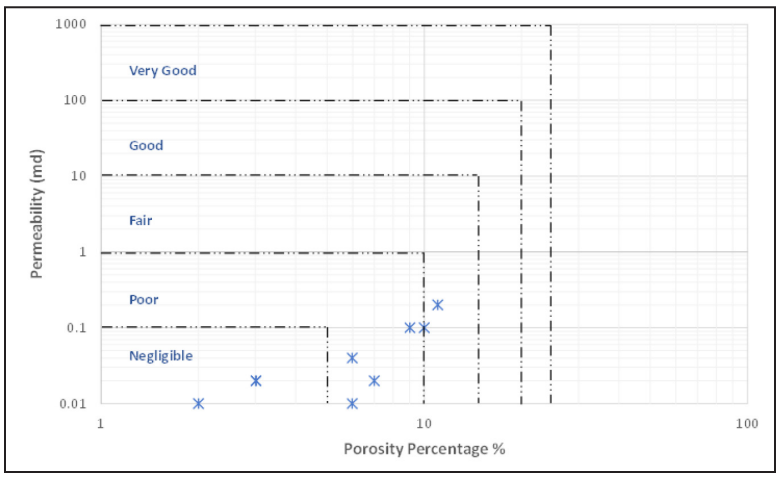

Figure 10: A scatter plot illustrates the relationship between porosity and permeability for samples from the Sarki Formation in the studied section. The plot is created using a qualitative classification of porosity and permeability derived from the descriptions provided by Levorsen (1967), North (1985), and Gluyas & Swarbrick (2004).

Ahmed, M.A., Nasser, M.E., & Jawad, S.N.A. 2020. Diagenesis processes impact on reservoir quality in carbonate Yamama Formation/Faihaa Oil field. Iraqi Journal of Science, 61(1), 92-102. https://doi.org/10.24996/ijs.2020.61.1.10.

Ahr, W.M., 2008. Geology of Carbonate Reservoirs: the identification, description, and characterization of hydrocarbon reservoirs in carbonate rocks. Texas A&M University, US. 296 p.

Al-Badry, A.M.S., 2012. Stratigraphy and geochemistry of Jurassic formations in selected sections – northern Iraq. PhD dissertation (unpublished), Science College, University of Baghdad, Baghdad, Iraq. 162 p.

Albeyati, F.M.O., Abdula, R.A. & Terzi, F., 2021. Porosity and permeability measurements integration of the upper Cretaceous in Balad Field, Central Iraq. Iraqi Geological Journal, 54(1B), 24-42. https://doi.org/10.46717/igj.54.1B.3Ms-2021-02-21.

Al-Dabagh, M.M. & Asaad, I.Sh., 2025. Investigation of Petrophysical Properties of Butmah Formation (Early Jurassic) Using Well Logs of Selected Wells, Northern Iraq. Iraqi National Journal of Earth Science, 25(2), In press. https://doi.org/10.33899/earth.2024.146079.1218.

Al-Juboury, A.I. & McCann, T., 2015. Petrological and geochemical interpretation of Triassic–Jurassic boundary sections from northern Iraq. Geological Journal, 50(2),157-172. https://doi.org/10.1002/gj.2537.

Anselmetti, F.S., Luthi, S. & Eberli, G.P., 1998. Quantitative characterization of carbonate pore systems by digital image analysis. AAPG Bulletin, 82(10),1815-1836.

Asaad, I.S., Balaky, S.M., Hasan, G.F. & Aswad, M.K., 2021. Sedimentology of the Baluti Formation (Late Triassic) in the Warte area, northeastern Iraqi Kurdistan region. Geological Journal, 56(8), 3923-3940. https://doi.org/10.1002/gj.4142.

Balaki, H.G., 2004. Geometry and structural history of Zozik-Rola and Spi Balies-Mama Ruta structures of the Zagros fold thrust belt in NE Iraqi Kurdistan. M.Sc. Thesis (unpublished), University of Salahadin, Iraq. 103 p.

Balaky, S.M., Al-Dabagh, M.M., Asaad, I.S., Tamar-Agha, M., Ali, M.S. & Radwan, A.E., 2023. Sedimentological and petrophysical heterogeneities controls on reservoir characterization of the Upper Triassic shallow marine carbonate Kurra Chine Formation, Northern Iraq: Integration of outcrop and subsurface data. Marine and Petroleum Geology, 149, 106085. https://doi.org/10.1016/j.marpetgeo.2022.106085.

Bellen, R.C., van, Dunnington, H.V., Wetzel, R. & Morton, D.M., 1959. Lexique Stratigraphique International. Asie, Fasc. 10a, Iraq, Paris. 333 p.

Buday, T., 1980. The Regional Geology of Iraq Vol. 1: Stratigraphy and Palaeogeography. Publications of GEOSURV., Baghdad. 445 p.

Choquette, P.W. & Pray, L.C., 1970. Geologic nomenclature and classification of porosity in sedimentary carbonates. AAPG Bulletin, 54(2), 207-250.

Delizy, B.A. & Shingaly, W.S., 2022. Microfacies Analysis and Depositional Environment of Sarki Formation (Early Jurassic), Rawanduz Area, Kurdistan Region, Northern Iraq. Tikrit Journal of Pure Science, 27(1), 24-35. https://doi.org/10.25130/tjps.v27i1.79.

Dunnington, H.V., 1958. Generation, Migration, Accumulation and Dissipation of Oil in Northern Iraq. In: Weeks, L.G. (Ed.), Habitite of Oil Symposium. American Association of Petroleum Geologists, New York, p.1194-1251.

Ehrlich, R., Kennedy, S.K., Crabtree, S.J. & Cannon, R.L., 1984. Petrographic image analysis; Analysis of reservoir pore complexes. Journal of Sedimentary Research, 54(4), 1365-1378. https://doi.org/10.1306/212F85DF-2B24-11D7-8648000102C1865D.

Fahad, M., Khan, M.A., Hussain, J., Ahmed, A. & Yar, M., 2021. Microfacies analysis, depositional settings and reservoir investigation of Early Eocene Chorgali formation exposed at eastern Salt Range, upper Indus basin, Pakistan. Carbonates and Evaporites, 36(3), 41. https://doi.org/10.1007/s13146-021-00708-7.

Gluyas, J. & Swarbrick, R., 2004. Petroleum Geoscience. Blackwell Publishing, Hoboken. 359 p.

Jassim, S.Z., Buday, T., Cicha, I. & Prouza, V., 2006. Late Permian-Liassic Megasequence AP6. In: Jassim & Goff (Eds.), Geology of Iraq. Dolin Prague and Moravian Museum, Brno. 352 p.

Jiang, Z., Quan, X., Tian, S., Liu, H., Guo, Y., Fu, X. & Yang, X., 2022. Permeability-Enhancing Technology through Liquid CO2 Fracturing and Its Application. Sustainability, 14(16), 10438. https://doi.org/10.3390/su141610438.

Levorsen, A.I.,1967. Geology of Petroleum. 2nd Edition, W.H. Freeman and Company, San Franciso, CA. 724 p.

Lunn, G. A., Miller, S. & Samarrai, A., 2019. Dating and correlation of the Baluti Formation, Kurdistan, Iraq: Implications for the regional recognition of a Carnian "marker dolomite", and a review of the Triassic to Early Jurassic sequence stratigraphy of the Arabian Plate. Journal of Petroleum Geology, 42(1), 5-36. https://doi.org/10.1111/jpg.12722.

Mohialdeen, I.M., Fatah, S.S., Abdula, R.A., Hakimi, M.H., Abdullah, W.H., Khanaqa, P.A. & Lunn, G.A., 2022. Stratigraphic correlation and source rock characteristics of the Baluti Formation from selected wells in the Zagros fold belt, Kurdistan Region, northern Iraq. Journal of Petroleum Geology, 45(1), 29-56. https://doi.org/10.1111/jpg.12806.

North, F.K., 1985. Petroleum Geology. Allen & Unwin, Boston. 607 p.

Omar, N., McCann, T., Al-Juboury, A.I., Franz, S.O., Zanoni, G. & Rowe, H., 2023. A comparative study of the paleoclimate, paleosalinity and paleoredox conditions of Lower Jurassic-Lower Cretaceous sediments in northeastern Iraq. Marine and Petroleum Geology, 156, 106430. https://doi.org/10.1016/j.marpetgeo.2023.106430.

Pirot, E.M. & Edilbi, A.N.F., 2022. Reservoir Characterization of Pila Spi Formation (Middle–Late Eocene) in Shaqlawa and Shekhan areas, Kurdistan Region, Northern Iraq. Tikrit Journal of Pure Science, 27(5), 29-39. https://doi.org/10.25130/tjps.v27i5.15.

Sissakian, V.K., 2000. Geological Map of Iraq (scale 1:1000000, 3rd edition) GEOSURVE. Baghdad, Iraq.

Surdashy, A.M., 1999. Sequence stratigraphic analysis of the Early-Jurassic, central and northern Iraq. Unpublished Ph.D. thesis, Baghdad University. 195 p.

Manuscript received 18 May 2024;
Received in revised form 12 August 2024;
Accepted 22 October 2024
Available online 30 May 2025